Journal of Chemical Health Risks

www.jchr.org

JCHR (2026) 16(2), 1106-1120 | ISSN:2251-6727

Green Synthesis and Physicochemical Characterization of Copper Oxide Nanoparticles Mediated by *Azadirachta indica* A. Juss. Leaf Extract

Rakesh Negi, Aradhana, Ruchi and Mukesh Kumar*

Department of Botany & Microbiology, Gurukula Kangri (Deemed to be University), Haridwar-249404 Uttarakhand, India

(Received: 16 January 2026 Revised: 25 February 2026 Accepted: 17 March 2026)

KEYWORDS

Azadirachta indica, Copper oxide nanoparticles (CuO NPs), FE-SEM, FTIR, GC-MS, XRD**,** Zeta Potential

ABSTRACT:

This study reports an eco-friendly and efficient method for the green synthesis of copper oxide nanoparticles (CuO NPs) using the aqueous leaf extract of *Azadirachta indica* A. Juss. Phytochemical profiling and GC–MS analysis of the extract revealed the presence of diverse bioactive compounds including fatty acid esters, alcohols, linoleic acid derivatives and andrographolide, which served as natural reducing and stabilizing agents during nanoparticle formation. The biosynthesized CuO NPs were characterized using UV–Vis, FTIR, XRD, FE-SEM, EDX, zeta potential and DLS analysis. UV–Vis spectroscopy confirmed nanoparticle formation with a characteristic absorption peak at 340 nm, attributed to electronic transitions in CuO nanoparticles. FTIR spectra verified the involvement of phenolics, flavonoids, terpenoids and other phytochemicals in reducing and capping the nanoparticles. XRD analysis confirmed the formation of highly crystalline monoclinic CuO phases. FE-SEM micrographs revealed spherical clustered nanoparticles with a mean size of 24.95 nm, while EDX confirmed high elemental purity containing only copper and oxygen. The zeta potential value of –21.4 mV indicated good colloidal stability due to biomolecule capping. The CuO nanoparticles exhibited a PDI value of 0.217, indicating monodispersity and acceptable colloidal stability of the dispersion. The findings demonstrate that *A. indica* leaf extract is an effective biological source for the green synthesis of stable CuO nanoparticles.

Introduction

Nanotechnology has emerged as a frontier of modern science, offering vast opportunities to manipulate matter at the nanoscale (1–100 nm) for developing materials with enhanced and tunable physicochemical properties. Metal oxide nanoparticles, in particular, have gained immense attention owing to their catalytic, optical, antimicrobial, therapeutic applications and electronic characteristics that differ significantly from their bulk counterparts [1]. Among various transition metal oxides, copper oxide (CuO) is a p-type semiconductor with a narrow bandgap (~1.7 eV) that exhibits remarkable electrical, thermal, and catalytic performance [2]. Owing to its low cost, abundance, and versatility, CuO nanoparticles (CuO NPs) have found extensive applications in photocatalysis, solar cells, gas sensors, batteries, antimicrobial coatings, and biomedical formulations [3].

Conventionally, CuO NPs have been synthesized using various physical and chemical methods such as sol–gel, precipitation, hydrothermal, sonochemical, and microwave-assisted routes [4]. Although these techniques allow precise control over particle size and morphology, they often involve expensive reagents, toxic solvents, and high energy inputs that raise concerns regarding environmental safety and sustainability. Furthermore, residual chemical impurities from these methods can limit the biocompatibility of the synthesized nanoparticles, restricting their direct use in medical and pharmaceutical applications [5].

To address these limitations, green synthesis also referred to as biogenic or phyto-assisted synthesis has emerged as a sustainable alternative that aligns with the principles of green chemistry. This approach utilizes natural biological systems such as plant extracts,

Journal of Chemical Health Risks
www.jchr.org
JCHR (2026) 16(2), 1106-1120 | ISSN:2251-6727

microorganisms, or biopolymers as reducing, capping, and stabilizing agents during nanoparticle formation [6]. Among these, plant-mediated synthesis is particularly attractive because it is simple, cost-effective, and suitable for large-scale production without requiring aseptic conditions or sophisticated instrumentation. Plant extracts contain diverse bioactive compounds including phenolics, flavonoids, terpenoids, tannins, saponins, alkaloids, and proteins, which act as both reducing and stabilizing agents, converting metal ions into stable nanoparticles through redox reactions [7].

Azadirachta indica A. Juss. (Neem) has been extensively studied for its pharmacological importance and rich phytochemical profile. The leaves of this plant contain a wide spectrum of bioactive constituents such as azadirachtin, nimbin, quercetin, and nimbolide, known for their antioxidant, antimicrobial, and metal-chelating properties. These compounds not only facilitate the reduction of copper ions (Cu^{2+}) into CuO NPs but also serve as natural stabilizers, preventing nanoparticle agglomeration and enhancing long-term stability. Green-synthesized CuO NPs using *A. indica* have demonstrated significant antibacterial, antifungal, and catalytic efficiencies as well as potential utility in energy storage and biomedical applications [8].

The mechanism of nanoparticle formation in plant-mediated synthesis generally involves the bioreduction of metal ions, followed by nucleation and growth controlled by phytochemicals. Reaction parameters such as extract concentration, temperature, pH, and precursor molarity strongly influence the physicochemical characteristics of the final product [1]. The functional groups present in plant metabolites such as hydroxyl, carboxyl, and carbonyl bind to the nanoparticle surface, providing electrostatic stability and facilitating uniform morphology [4]. Characterization techniques like UV visible spectroscopy, Fourier-transform infrared spectroscopy (FTIR), X-ray diffraction (XRD), and scanning electron microscopy (SEM) are essential to confirm nanoparticle formation, crystallinity, and surface modification.

In recent years, there has been a growing emphasis on integrating green nanotechnology with biomedicine, as biosynthesized metal oxide nanoparticles demonstrate enhanced compatibility, minimal toxicity, and strong bioactivity. CuO NPs, in particular, have shown potent antimicrobial efficacy against a broad range of pathogenic bacteria and fungi due to their ability to generate reactive oxygen species (ROS) and disrupt microbial membranes [3][7]. Additionally, their catalytic and semiconducting behavior makes them promising candidates for photocatalytic degradation of dyes, biosensors, and drug delivery systems [6].

The present research focuses on the green synthesis of copper oxide nanoparticles using the leaf extract of *Azadirachta indica A. Juss.*, aiming to develop an eco-friendly, low-cost, and sustainable method for nanoparticle fabrication. The synthesized CuO NPs were characterized by physicochemical techniques to elucidate their size, shape, structure, and surface chemistry. This study not only supports the concept of replacing conventional chemical synthesis with environmentally benign methods but also demonstrates the potential of *A. indica* as an effective biofactory for the sustainable production of CuO nanoparticles with promising biomedical and industrial applications.

Materials and Methods

Taxonomic Identification and Authentication of the Plant

For the present research work, the plant specimens of *Azadirachta indica* were collected from the main campus of Gurukula Kangri (Deemed to be University), Haridwar, U.K. The plant specimen was assigned a field number and pressed with the help of blotting paper sheets using wooden herbarium press. The herbarium specimen was deposited and taxonomically identified at Botanical Survey of India (BSI), Uttarakhand, India, where they were catalogued and assigned accession number for future reference.

Extraction of Plant Material

The leaves of *Azadirachta indica* A. Juss. were thoroughly washed with tap water followed by distilled water to remove dust particles. The leaves were shade-dried for two days and further the leaves were oven-dried at 40^{o}C to remove moisture contents from the leaves. Drying was necessary to remove moisture and enable long-term storage of the plant material. The dried plant material was pulverized and coarsely powdered by mechanical blender to obtain dried powdered form. The dried powder was stored at room temperature in airtight containers.

Journal of Chemical Health Risks
www.jchr.org
JCHR (2026) 16(2), 1106-1120 | ISSN:2251-6727

Soxhlet Extraction

The powdered plant material (50 g) was successively extracted using solvents of increasing polarity- ethyl acetate, ethanol, methanol, and distilled water through Soxhlet extraction. Each extraction was carried out with 250 mL of solvent for 12–14 hours until the siphon solvent turned colorless, indicating complete extraction. The obtained extracts were concentrated using hot air oven under controlled temperature (60-70^{o}C) for 24 hrs to yield a semi-solid mass. These residues were dried in petri plates for complete solvent removal and stored in labeled airtight containers for further qualitative phytochemical screening [9].

Phytochemical Screening

Qualitative Phytochemical Analysis

The crude leaves extracts were subjected to standard qualitative tests for the detection of major phytoconstituents using established procedures from previous studies. The methods and corresponding references are summarized in Table 1.

Table 1. Standard qualitative tests for detection of phytoconstituents in leaves extracts

Phytochemical	Test / Procedure	Observation	References
Tannins	2 ml of extract was mixed with a few drops of 1% ferric chloride solution.	Formation of blue-green precipitate confirms tannins.	[10]
Alkaloids	0.5 g of sample was dissolved in 1% HCl, filtered, and 2 ml of filtrate treated with Dragendorff's reagent (potassium bismuth iodide).	Red or orange precipitate indicates alkaloids.	[10]
Phenols	10 mg extract was treated with a few drops of lead acetate solution.	Yellow-colored precipitate confirms phenols.	[11]
Saponins	0.5 mg extract was shaken vigorously with 5 ml distilled water.	Stable froth formation indicates saponins.	[11]
Glycosides	5 ml extract mixed with 0.3 ml each of Fehling's A and B solutions until the mixture turned alkaline.	Brick-red coloration confirms glycosides.	[10]
Amino acids	1 ml extract treated with a few drops of Ninhydrin reagent.	Purple coloration indicates amino acids.	[12]
Steroids	2 ml extract dissolved in chloroform, followed by 2 ml concentrated H_2SO_4.	Red coloration confirms steroids.	[13]
Flavonoids	5 ml extract mixed with 0.1 g metallic zinc and 8 ml concentrated H_2SO_4.	Red coloration indicates flavonoids.	[11]
Coumarins	3 ml of 10% NaOH added to aqueous extract.	Yellow coloration confirms coumarins.	[14]

Quantitative and GC–MS Analysis

Among all solvent extracts, the one showing maximum phytochemical richness was selected for GC–MS analysis. Gas chromatography–mass spectrometry (Shimadzu QP 2010 Ultra, Japan) was performed using helium as the carrier gas (flow rate 1.0 mL/min), with an injection volume of 1 µL, and oven-temperature program from 70°C to 310°C at 5°C min^{-1}. Mass spectra were recorded over m/z 40–850 and compounds were identified by comparison with the Wiley spectral library.

Journal of Chemical Health Risks
www.jchr.org
JCHR (2026) 16(2), 1106-1120 | ISSN:2251-6727

Green Synthesis of CuO Nanoparticles

The green copper oxide nanoparticles (g-CuO NPs) were synthesized using copper nitrate trihydrate ($Cu(NO_3)_2 \cdot 3H_2O$) as a precursor and *Azadirachta indica* leaf extract as a reducing and capping agent. The synthesized nanoparticles were then centrifuged at 25,000 rpm and washed thoroughly with deionized water and ethanol to remove unreacted components, followed by sonication in an ultrasonic bath to ensure uniform dispersion. Subsequently, the dried nanoparticles were subjected to calcination in a muffle furnace at 400–500°C for 2 h to obtain pure crystalline g-CuO NPs. The final product was characterized using UV, FTIR, XRD, FE-SEM, EDX, DLS and Zeta potential analysis [2].

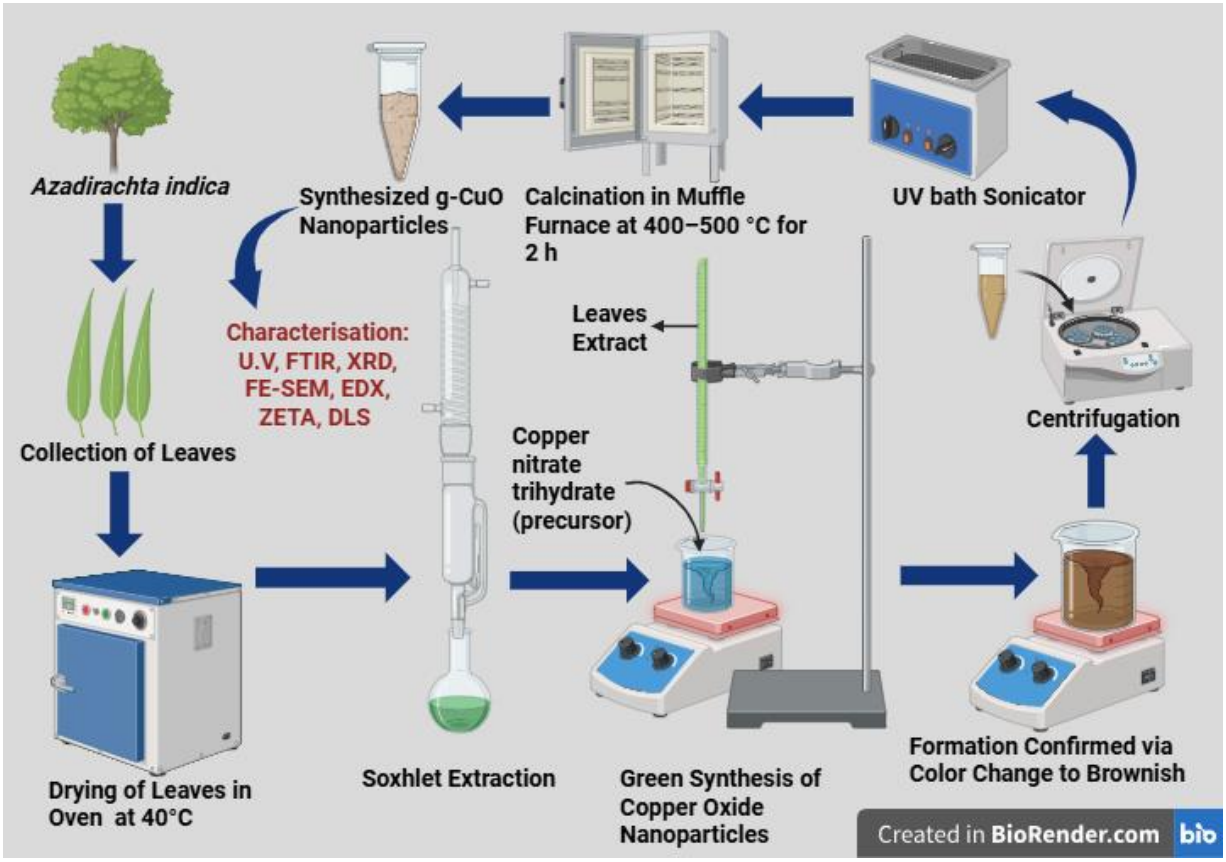

Fig. 1 Graphical representation of green synthesis of CuO nanoparticles

Characterization of Green Synthesized Copper Oxide Nanoparticles

UV–Visible Spectroscopy

It is a vital procedure that confirms the synthesis and stability of metal nanoparticles in aqueous solution. The absorption in the visible spectrum was measured with systronics double beam UV-visible spectrophotometer (Shimadzu UV-1800) having wavelength range of 200-800 nm to confirm nanoparticle formation.

Fourier Transform Infrared Spectroscopy (FTIR) Analysis of synthesized Copper Oxide nanoparticles

FTIR spectroscopy was used to identify functional groups responsible for reduction and stabilization of biosynthesized nanoparticles. Spectra were recorded using a Bruker Tensor 27 spectrometer in the range of 400–4000 cm^{-1} at a resolution of 4 cm^{-1}. Characteristic absorption peaks were analyzed to determine the functional groups involved in nanoparticle formation and capping.

Journal of Chemical Health Risks
www.jchr.org
JCHR (2026) 16(2), 1106-1120 | ISSN:2251-6727

X-Ray Diffraction (XRD) Analysis of synthesized Copper Oxide nanoparticles

In XRD process X-rays are passed through a nanoparticle that produces a pattern indicating the information about their size and shape. Using powder X-ray diffraction technique, the crystal structure of the nanoparticles was analysed. XRD patterns were recorded on an automated analytical X'Pert Pro-X-ray diffractometer with Cu Kα radiation (λ = 1.5406 Å). The samples were scanned over a 2θ range of 20°–80° at room temperature. Crystallite size was estimated by the Debye–Scherrer equation.

Field Emission Scanning Electron Microscopy (FE-SEM) and Energy Dispersive X-Ray (EDX) Analysis

The shape, size and morphological features at different magnifications of synthesized nanoparticles were elucidated with the help of FEI Nova NanoSEM 450 FE-SEM. A beam energy of 10 kV was used for SEM analysis. The equipment was equipped with an EDX source to detect the elemental details of the synthesized NPs.

Zeta Potential (ZP) and Dynamic Light Scattering (DLS)

The Malvern-Zetasizer Nano ZSP (ZEN 5600) instrument was used to analyze the particle size zeta potential using a zeta dip cell. The charges on the surface of the synthesised copper nanoparticles and their stability were ascertained by calculating their zeta potential. Greater zeta potential values signify repulsive forces that prevent nanoparticles from aggregating and promote particle stability [15]. The value of zeta potential gives the degree of electrostatic repulsion between adjacent, similarly charged particles in the dispersion.

DLS were used to measure the mean particle size and charge on the surface of nanoparticles. DLS results were based on the hydrodynamic diameter of NPs synthesized in which NPs were dissolved in a dispersant and responsible for forming noncovalent interactions, causing the particle size to be bigger than SEM and TEM techniques. The PDI values were used to evaluate the homogeneity of the colloidal dispersion. A PDI range of 0.01 to 0.5–0.7 indicates monodispersed nanoparticle systems, whereas values greater than 0.7 signify a highly polydispersed nature of the prepared particles.

Results and Discussion

Taxonomic Authentication

The plant material used for the study was identified and authenticated as *Azadirachta indica* A. Juss. (Family: Meliaceae; Accession No. 1632) at the Botanical Survey of India, Dehradun, Uttarakhand. Proper authentication ensures the botanical accuracy and reliability of the research outcomes, as misidentification can significantly alter the phytochemical and pharmacological interpretation of results.

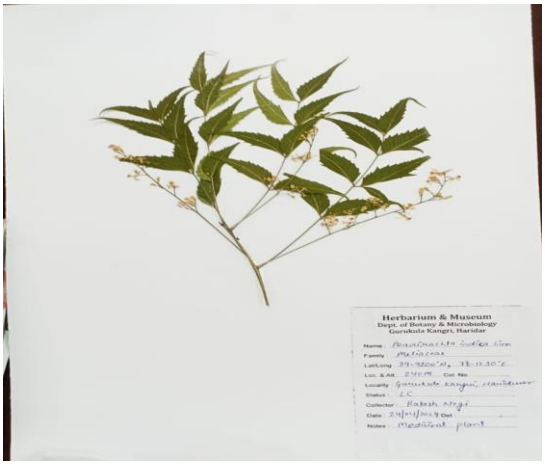

Fig. 2 Herbarium Specimen of *Azadirachta indica*

Fig. 3 Herbarium authentication certificate issued by

Journal of Chemical Health Risks

www.jchr.org

JCHR (2026) 16(2), 1106-1120 | ISSN:2251-6727

A. Juss.

Phytochemical Screening

The qualitative phytochemical analysis of *Azadirachta indica* extracts prepared in four solvents-ethyl acetate, ethanol, methanol, and distilled water revealed distinct solubility profiles of secondary metabolites (Table 2). Flavonoids were found in all extracts, indicating their broad solubility and abundance in neem leaves. Tannins, amino acids, and coumarins were detected in ethanol and distilled water, while phenols and glycosides were observed in methanol and distilled water. Saponins were present in all solvents except ethanol, whereas alkaloids and steroids were exclusively present in the aqueous extract [16].

The higher diversity of phytochemicals in the distilled water extract suggests that water is an effective solvent for extracting polar bioactive compounds from *A. indica*. These compounds are known to contribute to the plant's pharmacological properties, including antimicrobial, antioxidant, and anti-inflammatory activities. Therefore, the aqueous extract was selected for further GC–MS analysis to identify specific bioactive constituents.

Table 2. Qualitative Phytochemical Analysis of *Azadirachta indica*

S.No.	Phytochemicals	Solvents			
		Ethyl acetate	Ethanol	Methanol	Dist. Water
1.	Tannins	-	+	-	+
2.	Alkaloids	-	-	-	+
3.	Phenol	-	-	+	+
4.	Glycosides	-	-	+	-
5.	Saponins	+	-	+	+
6.	Steroids	-	-	-	+
7.	Amino acids	-	+	-	+
8.	Coumarin	-	+	-	+
9.	Flavonoids	+	+	+	+

GC-MS of leaves extract of *Azadirachta indica* in distilled water

The GC–MS chromatogram of the aqueous leaf extract of *Azadirachta indica* revealed multiple well-resolved peaks corresponding to a diverse range of bioactive phytoconstituents (Fig. 4; Table 3). Compound identification was carried out by comparing mass spectra with the NIST library database, and only compounds with high spectral similarity and chemically plausible matches were considered. The major compounds identified were Z,E-2,13-octadecadien-1-ol (10.00%),(Z,Z)-6,9-pentadecadien-1-ol (8.47%), glycidyl palmitoleate (6.01%), linoleic acid ethyl ester (4.93%), 17-octadecynoic acid (4.93%), 6-octadecenoic acid (4.57%) and andrographolide (4.07%). The predominance of long-chain unsaturated fatty alcohols, fatty acid derivatives, and diterpenoid constituents indicates a lipid-rich and chemically diverse extract.

Unsaturated fatty acids and their esters, such as linoleic acid derivatives and octadecenoic acid, are known to exhibit significant antimicrobial, anti-inflammatory, and antioxidant properties. Andrographolide, a diterpenoid lactone, has been extensively reported for its immunomodulatory, antioxidant, and therapeutic potential. The presence of such bioactive constituents supports the pharmacological relevance of *A. indica* and corroborates its extensive traditional use in herbal medicine. Furthermore, the GC–MS profile revealed a

Journal of Chemical Health Risks
www.jchr.org
JCHR (2026) 16(2), 1106-1120 | ISSN:2251-6727

substantial abundance of oxygenated hydrocarbons, fatty acid esters, and alcohol derivatives bearing hydroxyl and carboxyl functional groups. These functional moieties are capable of acting as effective electron donors and surface-stabilizing agents, thereby facilitating the reduction of copper ions and subsequent stabilization of CuO nanoparticles. Thus, the phytochemical composition of the aqueous leaf extract plays a crucial role in the green synthesis, reduction and capping involved in CuO NP formation.

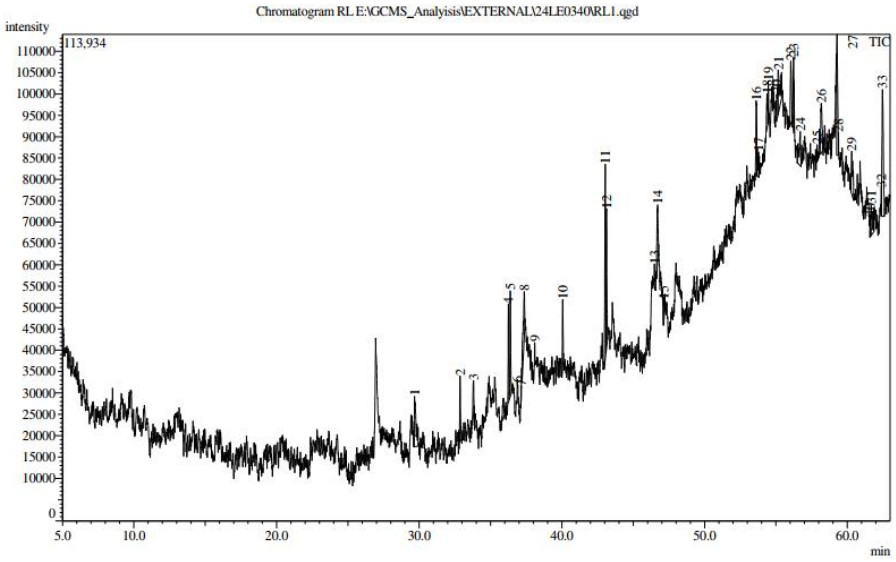

Fig. 4 Graphical representation of GC-MS of leaves extract of *Azadirachta indica* in distilled water

Table 3. GC-MS data of leaves extract of *Azadirachta indica* A. Juss. in distilled water

S.No	RT (min)	Area %	Identified compound	Molecular Formula
1	32.863	2.38	Pentadecanoic acid, 14-methyl-, methyl ester	$C_{16}H_{32}O_2$
2	33.806	1.87	8-Methylnonanoic acid	$C_{10}H_{20}O_2$
3	36.253	3.36	9,12-Octadecadienoic acid, methyl ester (E,E)	$C_{19}H_{34}O_2$
4	36.382	4.57	6-Octadecenoic acid, methyl ester (Z)	$C_{19}H_{36}O_2$
5	36.875	0.03	Heptacosanoic acid, methyl ester	$C_{28}H_{56}O_2$
6	37.358	4.93	17-Octadecynoic acid	$C_{18}H_{32}O_2$
7	40.055	2.72	Glycidyl palmitate	$C_{19}H_{36}O_3$
8	43.037	8.47	(Z,Z)-6,9-Pentadecadien-1-ol	$C_{15}H_{26}O$
9	43.125	6.01	Glycidyl palmitoleate	$C_{19}H_{34}O_3$
10	46.475	0.83	9,12-Octadecadienoyl chloride (Z,Z)	$C_{18}H_{31}ClO$
11	46.710	3.97	2-Methyl-Z,Z-3,13-octadecadien-1-ol	$C_{19}H_{36}O$
12	47.133	0.91	3-(Hexadecyloxy)propan-1-ol	$C_{19}H_{40}O_2$

Journal of Chemical Health Risks
www.jchr.org
JCHR (2026) 16(2), 1106-1120 | ISSN:2251-6727

S.No	RT (min)	Area %	Identified compound	Molecular Formula
13	53.616	4.07	Andrographolide	$C_{20}H_{30}O_5$
14	53.783	1.62	12-Methyl-E,E-2,13-octadecadien-1-ol	$C_{19}H_{36}O$
15	54.375	1.85	5-Cyclohexadecen-1-one	$C_{16}H_{28}O$
16	55.165	4.93	Linoleic acid ethyl ester	$C_{20}H_{36}O_2$
17	56.044	3.96	Panaxjapyne A	$C_{17}H_{26}O$
18	56.230	2.96	Z,Z,Z-1,4,6,9-Nonadecatetraene	$C_{19}H_{32}$
19	59.383	0.23	Cis-2,5-dimethylthiane	$C_7H_{14}S$
20	60.306	3.46	5,8,11-Heptadecatrien-1-ol	$C_{17}H_{30}O$
21	61.608	0.62	Cyclohexene, 3-(1-methylpropyl)-	$C_{10}H_{18}$
22	62.383	0.75	Trifluoroacetyl-α-terpineol	$C_{12}H_{17}F_3O_2$
23	62.469	10.00	Z,E-2,13-Octadecadien-1-ol	$C_{18}H_{34}O$

Green Synthesis of CuO Nanoparticles

Copper oxide nanoparticles (CuO NPs) were synthesized using the aqueous leaf extract of *A. indica* as a bioreducing and capping agent. The visible colour change from blue to dark brown indicated the formation of CuO nanoparticles (Fig. 5). This color transition is attributed to the reduction of Cu^{2+} ions to CuO by the phytochemicals present in the extract, primarily flavonoids, phenols and terpenoids. *Azadirachta indica* contains several complex phytochemicals which actively participate in the reduction of metal ions during nanoparticle formation. During biosynthesis, these biomolecules act as natural stabilizing agents by forming a protective layer around the nanoparticle surface.

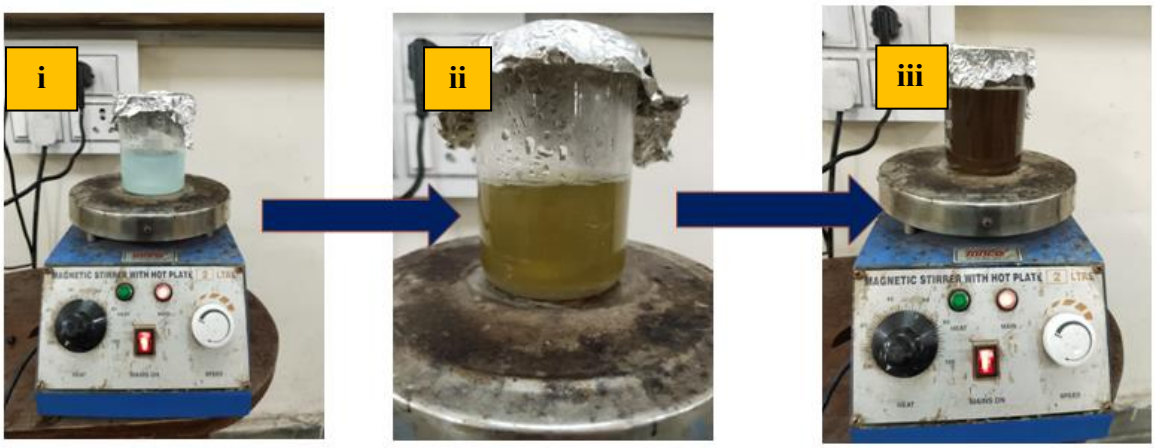

Fig. 5 Stepwise visual color transformation observed during the green synthesis of CuO nanoparticles: (i) copper nitrate precursor solution, (ii) reaction mixture with *Azadirachta indica* extract under heating and stirring, and (iii) final dark brown colloidal suspension confirming successful formation of CuO NPs.

Journal of Chemical Health Risks
www.jchr.org
JCHR (2026) 16(2), 1106-1120 | ISSN:2251-6727

Characterization of Green Synthesized CuO Nanoparticles

UV-Visible spectroscopy

UV–Vis spectroscopy confirmed the synthesis and colloidal stability of the nanoparticles. The UV-visible absorbance spectrum recorded for CuO NPs exhibited λ_{max} of 340 nm (Fig. 6). The absorption peak at 340 nm corresponds to electronic transitions in CuO nanoparticles. UV–Vis analysis qualitatively confirms nanoparticle formation [17] [18].

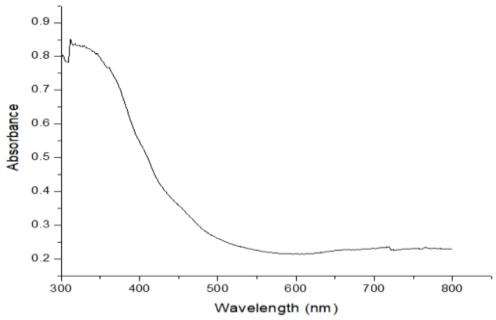

Fig. 6 UV-Vis graph of CuO Nanoparticles

Fourier Transform Infrared Spectroscopy (FTIR) Spectral Analysis

The FTIR spectrum of the green-synthesized CuO nanoparticles showed characteristic peaks at 3728, 3110, 2128, 1675, 1457, 1091, 745, 597, and 523 cm^{-1} (Fig. 7). The peak observed at 3110 cm^{-1} corresponds to the O–H stretching vibration of phenolic groups present in the *Azadirachta indica* extract, indicating their role in reduction and capping. The band at 2128 cm^{-1} is attributed to C–N stretching of aromatic amines, while the absorptions at 1675 and 1457 cm^{-1} represent C=O and C=C vibrations of phytoconstituents such as flavonoids and terpenoids. The peak around 1091 cm^{-1} corresponds to C–O stretching, characteristic of ether or alcohol functional groups, suggesting the involvement of polysaccharides or polyphenols in nanoparticle stabilization. Additionally, the strong bands observed at 597 and 523 cm^{-1} are assigned to Cu–O stretching vibrations, confirming the successful formation of copper oxide nanoparticles and their interaction with biomolecules from the plant extract [19] [5].

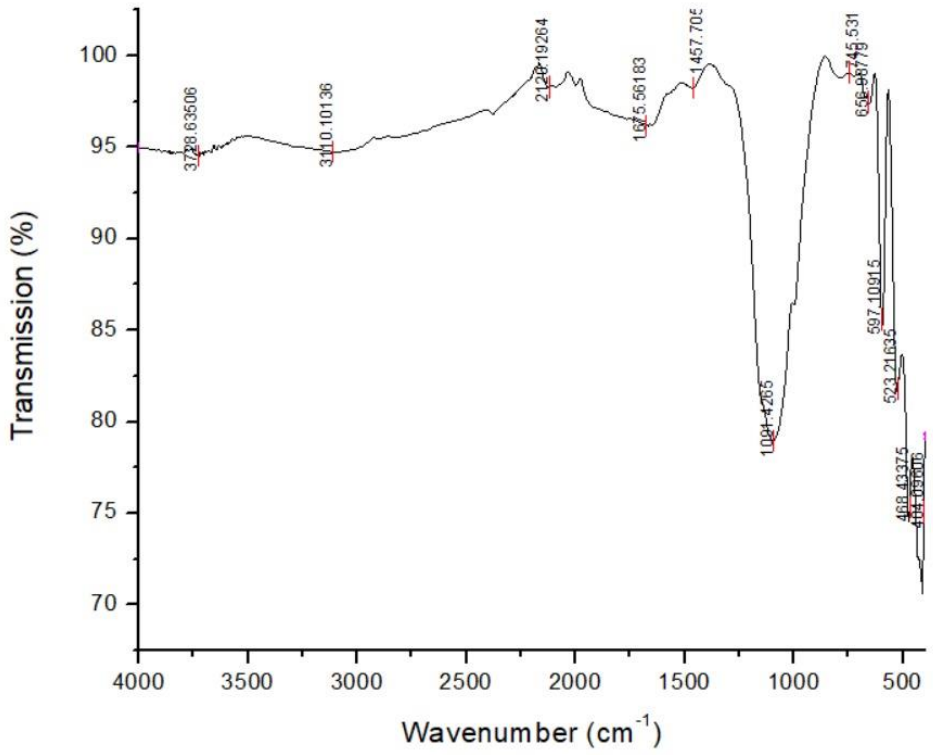

Fig. 7 FTIR Spectrum of *Azadirachta indica* mediated synthesized Copper Oxide nanoparticles

Journal of Chemical Health Risks
www.jchr.org
JCHR (2026) 16(2), 1106-1120 | ISSN:2251-6727

X-ray Diffraction Analysis of synthesized Copper Oxide nanoparticles

The XRD analysis was performed at room temperature with a scanning rate of 20 min^{-1} from 20° to 80° (Fig. 8). The observed diffraction sharp peaks position at 2θ= (32.69°, 35.65°, 38.95°, 49.00°, 53.61°, 58.48°, 61.69°, 66.39°, 68.29°, 72.57° and 75.37° were assigned to (110), (-111), (111), (-2 02), (020), (202), (-113), (-311), (220), (311) and (-222) are highly consistent with JCPDS standard no. 01-080-0076 of CuO NPs. No diffraction peaks corresponding to any impurities were observed, indicating that the XRD pattern confirms the successful formation of pure copper oxide nanoparticles [20] [21].

The average particle sizes of the nanoparticles were calculated from FWHM using the Scherrer's equation. The Debye-Scherrer equation states that D = kλ/ β cosθ, where D is particle size (nm), k is a constant of 0.94, λ is the wavelength of the X-ray source (0.15406 nm), β is the full width at half maximum (FWHM) and θ is the half diffraction angle, Bragg angle (degree). The average crystallite size was calculated using the Debye–Scherrer equation and found to be 17.012 nm.

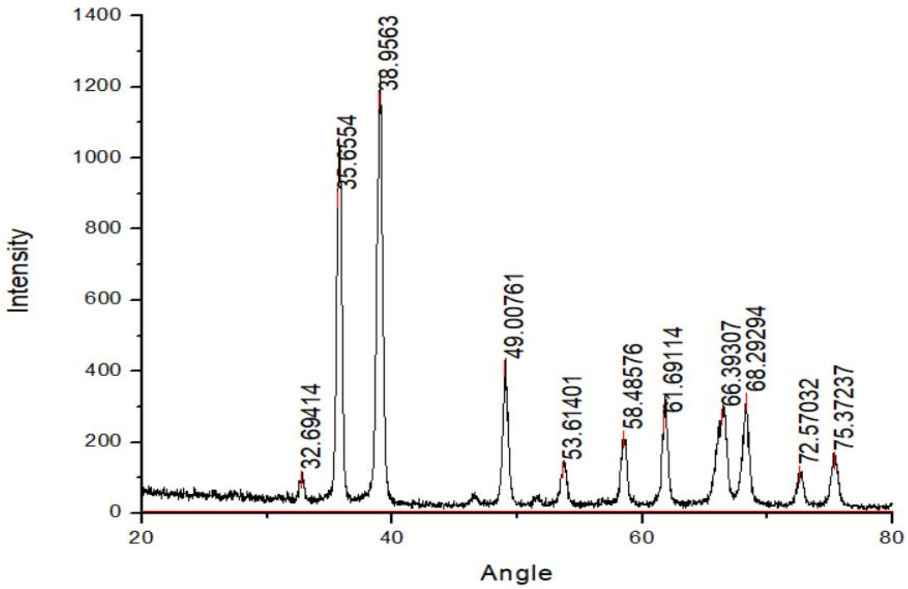

Fig. 8 XRD patterns of *Azadirachta indica* mediated synthesized Copper Oxide nanoparticles

Field Emission Scanning Electron Microscope (FE-SEM) and Energy Dispersive X-ray (EDX) Analysis of synthesized Copper Oxide nanoparticles

FE-SEM images revealed the formation of spherical, clustered nanostructures with a mean size of 24.95nm. The micrographs also demonstrated the presence of certain bigger particles due to agglomeration, with more or less consistent size, shape, and morphology (Fig. 9 a-b). This behavior is attributed to the tendency of nanoparticles to aggregate in order to lower Gibbs free energy, coupled with electrostatic interactions between the surface-associated bio-organic capping molecules. Since the synthesis involves plant-derived materials, the presence of atmospheric moisture also promotes the clustering of smaller nanoparticles [22].

Journal of Chemical Health Risks
www.jchr.org
JCHR (2026) 16(2), 1106-1120 | ISSN:2251-6727

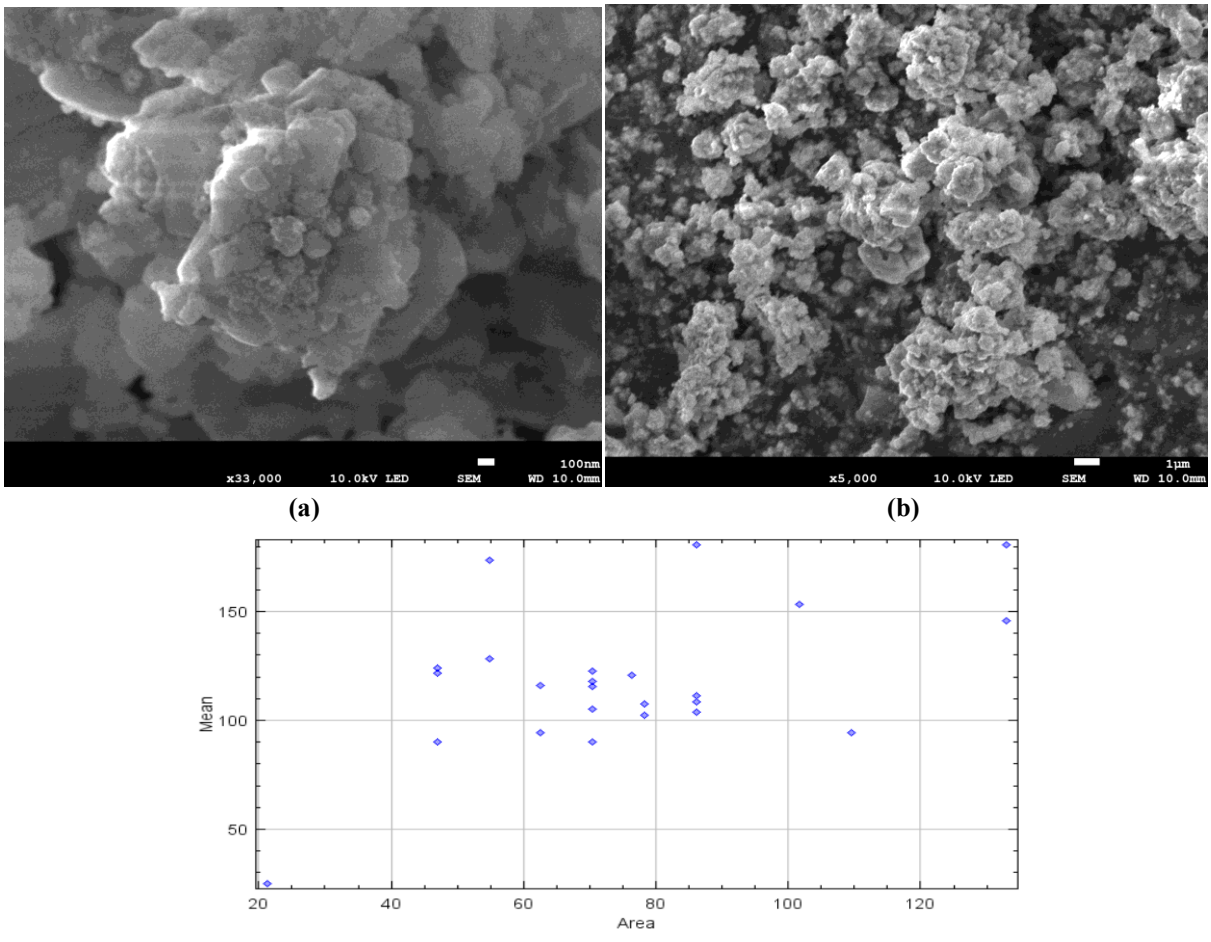

Fig 9. (a-b) FE-SEM micrograph of the green synthesized CuO NPs, c) Correlation between particle area and mean particle size of CuO nanoparticles determined from FE-SEM analysis

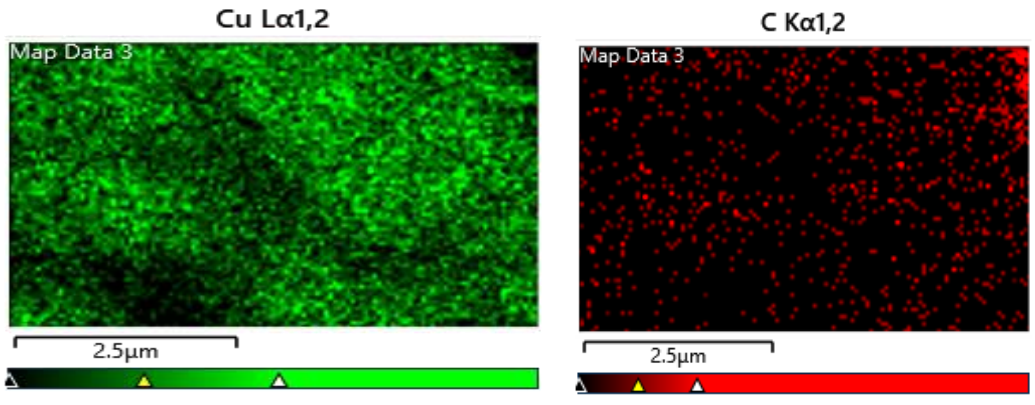

Fig 10. (a-d): Electron mapping

The chemical composition of the NPs was studied by EDX analysis. The peaks corresponding to elemental Cu and O were clearly identified, and no additional peaks were present, indicating the high purity of the synthesized nanoparticles and this was consistent with the XRD studies (Fig. 11) [23].

Journal of Chemical Health Risks
www.jchr.org
JCHR (2026) 16(2), 1106-1120 | ISSN:2251-6727

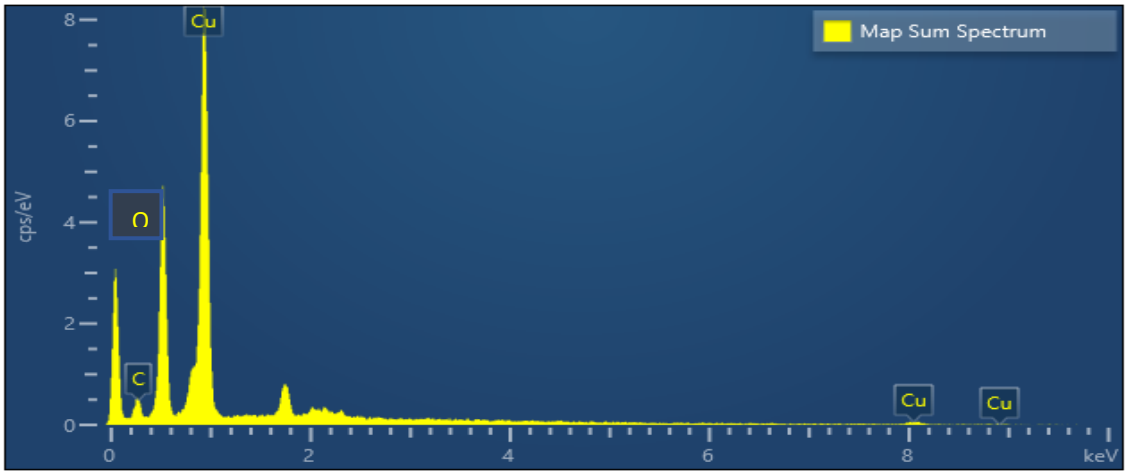

Fig. 11 EDX graph of green synthesized CuO nanoparticles

Zeta Potential, Size distribution and PDI

The zeta potential of synthesized copper nanoparticles at pH 7 is negative in the present study, which may be attributed to the capping of nanoparticles by plant biomolecules. Synthesized copper nanoparticles showed a zeta potential sharp peak at of -21.4mV (Fig. 12) with a conductivity of 0.113 mS/cm suggesting moderate colloidal stability of the biosynthesized nanoparticles [24].

The particle size observed by FE-SEM was approximately 24.95 nm, representing the primary size of the nanoparticles in the dry state. Notably, the particle size distribution obtained from DLS was significantly larger than the core particle size observed by FE-SEM and that estimated by XRD. This increase in size can be attributed to particle aggregation in the aqueous medium, along with the presence of a hydration layer and surface-bound bio-organic capping molecules surrounding the g-CuONPs. The average hydrodynamic diameter of the CuO nanoparticles was found to be 320 nm with a polydispersity index (PDI) of 0.217 (Fig. 13), indicating moderate dispersion and acceptable colloidal stability [25].

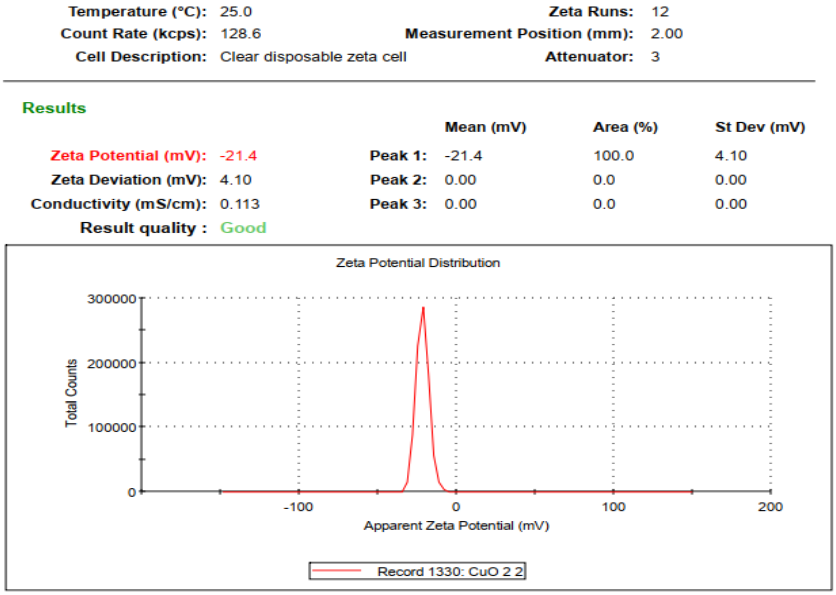

Fig 12. Zeta Potential graph of green synthesized CuO nanoparticles

Journal of Chemical Health Risks
www.jchr.org
JCHR (2026) 16(2), 1106-1120 | ISSN:2251-6727

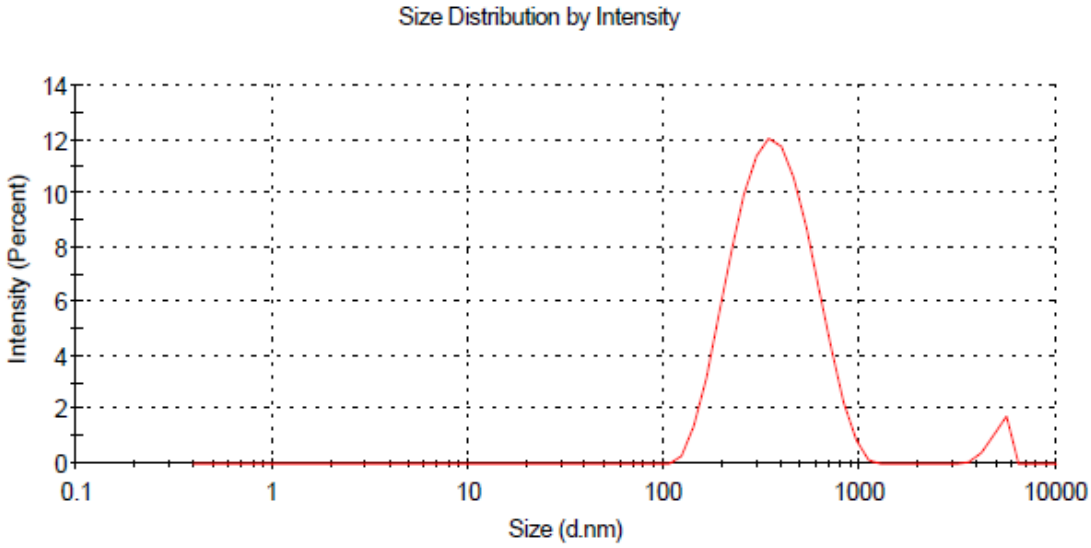

Fig 13. Particle size distribution graph of green synthesized CuO nanoparticles

Conclusion

This study demonstrates that the aqueous leaf extract of *Azadirachta indica* can serve as a natural, low-cost, and sustainable reducing and capping agent for the synthesis of copper oxide nanoparticles. The rich phytochemical composition of the extract played a crucial role in converting copper ions into stable CuO nanostructures without the use of toxic chemicals or high-energy inputs, supporting the principles of green chemistry. Comprehensive characterization confirmed the formation of pure, good crystalline, nanoscale dimensions with high elemental purity, moderate colloidal stability and efficient surface modification by bio-organic compounds. Overall, the work validates *A. indica* as a promising biological source for nanoparticle fabrication and provides a reliable platform for potential applications in antimicrobial coatings and biomedical formulations, catalysis and energy-related technologies.

Acknowledgement

The authors are grateful to the Head, Department of Botany and Microbiology Gurukula Kangri (DU), for providing the necessary laboratory facilities to carry out this research work. We sincerely acknowledge the financial assistance (Sanction Letter No-UCS&T/R&D-22/22-23/21211/1 Dated 16-06-2022) provided by the Uttarakhand State Council for Science and Technology (UCOST), Dehradun, which greatly contributed to the successful completion of this research work. We acknowledge the Department of Pharmaceutical Sciences, Gurukula Kangri (DU), for UV Spectroscopy and sonicator facilities. Acknowledgment is extended to Botanical Survey of India (BSI), Dehradun, for providing taxonomic identification and authentication of the collected plant specimen. The authors further acknowledge the CIL, Central University of Punjab, Bathinda for GC-MS, FTIR and XRD facilities, MNIT, Jaipur for providing Zeta potential, DLS and PR Testing Services India for FESEM, EDS and mapping facilities.

Conflict of Interest

The authors declare that there is no conflict of interest regarding this research work.

References

1. Waris, A., Din, M., Ali, A., Afridi, S., Baset, A., & Khan, A. U. 2021. *A comprehensive review of green synthesis of copper oxide nanoparticles and their diverse biomedical applications. Inorganic Chemistry Communications, 123*, 108369. https://doi.org/10.1016/j.inoche.2020.108369

2. Chakraborty, N., Banerjee, J., Chakraborty, P., Banerjee, A., Chanda, S., Ray, K., Acharya, K., & Sarkar, J. 2022. *Green synthesis of copper/copper oxide nanoparticles and their applications: A review. Green Chemistry Letters and Reviews, 15*(1),

Journal of Chemical Health Risks

www.jchr.org

JCHR (2026) 16(2), 1106-1120 | ISSN:2251-6727

187–215. https://doi.org/10.1080/17518253.2022.2025916

3. Vijay Kumar, P. P. N., Shameem, U., Kollu, P., Kalyani, R. L., & Pammi, S. V. N. 2015. *Green synthesis of copper oxide nanoparticles using Aloe vera leaf extract and its antibacterial activity against fish bacterial pathogens. BioNanoScience, 5*, 135–139. https://doi.org/10.1007/s12668-015-0171-z

4. Vishveshvar, K., Krishnan, M. V. A., Haribabu, K., & Vishnuprasad, S. 2018. *Green synthesis of copper oxide nanoparticles using Ixora coccinea plant leaves and its characterization. BioNanoScience, 8*, 554–558. https://doi.org/10.1007/s12668-018-0508-5

5. Padil, V. V. T., & Černík, M. 2013. *Green synthesis of copper oxide nanoparticles using gum karaya as a biotemplate and their antibacterial application. International Journal of Nanomedicine, 8*, 889–898. https://doi.org/10.2147/IJN.S40599

6. Akintelu, S. A., Folorunso, A. S., Folorunso, F. A., & Oyebamiji, A. K. 2020. *Green synthesis of copper oxide nanoparticles for biomedical application and environmental remediation. Heliyon, 6*(7), e04508. https://doi.org/10.1016/j.heliyon.2020.e04508

7. Sharma, B. K., Shah, D. V., & Roy, D. R. 2018. *Green synthesis of CuO nanoparticles using Azadirachta indica and its antibacterial activity for medicinal applications. Materials Research Express, 5*(9), 095033. https://doi.org/10.1088/2053-1591/aad91d

8. Ikhioya, I. L., Nkele, A. C., & Ochai-Ejeh, F. U. 2024. *Green synthesis of copper oxide nanoparticles using neem leaf extract (Azadirachta indica) for energy storage applications. Materials Research Innovations, 28*(3), 214–220. https://doi.org/10.1080/14328917.2023.2252677

9. Hashim, N., Abdullah, S., Hassan, L. S., Ghazali, S. R., & Jalil, R. 2021. A study of neem leaves: Identification of method and solvent in extraction. *Materials Today: Proceedings*, *42*, 217-221.

10. Ujah, I.I., Nsude, C.A., Ani, O.N., Alozieuwa, U.B., Okpako, I.O. and Okwor, A.E. 2021. Phytochemicals of Neem plant (*Azadirachta indica*) explains its use in traditional medicine and pest control. *GSC Biological and Pharmaceutical Sciences*, 14, 265-171.

11. Santhi, K. and Sengottuvel, R. 2016. Qualitative and quantitative phytochemical analysis of *Moringa concanensis* Nimmo. *International Journal of Current Microbiology and Applied Sciences*, 5(1), 633-640.

12. Al-Hashemi, Z.S.S. and Hossain, M.A. 2016. Biological activities of different Neem leaves crude extracts used locally in Ayurvedic medicine. *Pacific Science Review A: Natural Science and Engineering*, 18(2), 128-131.

13. Raphael, E. 2012. Phytochemical constituents of some leaves extract of *Aloe vera* and *Azadirachta indica* plant species. *Global Advanced Research Journal of Environmental Science and Toxicology*, 1(2), 014-017.

14. Le Thi, V.A., Nguyen, N.L., Nguyen, Q.H., Van Dong, Q., Do, T.Y. and Nguyen T, K.O. 2021. Phytochemical Screening and Potential Antibacterial Activity of Defatted and Nondefatted Methanolic Extracts of Xao Tam Phan (*Paramignya trimera* (Oliv.) Guillaum) Peels against Multidrug-Resistant Bacteria. *Scientifica*, 2021(1), 4233615.

15. Varadavenkatesan, T., Selvaraj, R., & Vinayagam, R. 2016. Phyto-synthesis of silver nanoparticles from Mussaenda erythrophylla leaf extract and their application in catalytic degradation of methyl orange dye. *Journal of Molecular Liquids*, *221*, 1063-1070.

16. Ruchi, & Kumar, M. 2024. Antibacterial and anti-inflammatory potential of Azadirachta indica against dental bacteria. *Environment Conservation Journal*, *25*(4), 1140–1149. https://doi.org/10.36953/ECJ.28952911

17. Devadoss, D., Asirvatham, A., Kujur, A., Saaron, G., Devi, N., & Mary, S. J. 2023. Green synthesis of copper oxide nanoparticles from Murraya koenigii and its corrosion resistivity on Ti-6Al-4V dental alloy. *Journal of the Mechanical Behavior of Biomedical Materials*, *146*, 106080.

18. Teklu, B., Kadiri, S. K., & Vidavalur, S. 2023. Green synthesis of copper oxide nanoparticles using

Balanites aegyptiaca stem bark extract and investigation of antibacterial activity. *Results in Chemistry*, *6*, 101152.

19. Rehana, D., Mahendiran, D., Kumar, R. S., & Rahiman, A.K. 2017. Evaluation of antioxidant and anticancer activity of copper oxide nanoparticles synthesized using medicinally important plant extracts. *Biomedicine & Pharmacotherapy*, *89*, 1067-1077.
20. Basith, N. M., Vijaya, J. J., Kennedy, L. J., & Bououdina, M. 2014. Structural, morphological, optical, and magnetic properties of Ni-doped CuO nanostructures prepared by a rapid microwave combustion method. *Materials science in semiconductor processing*, *17*, 110-118.
21. Patterson, A.L. 1939. The Scherrer formula for X-ray particle size determination. *Physical review*, *56*(10), 978.
22. Ananth, A., Dharaneedharan, S., Heo, M. S., & Mok, Y.S. 2015. Copper oxide nanomaterials: Synthesis, characterization and structure-specific antibacterial performance. *Chemical Engineering Journal*, *262*, 179-188.
23. Abbas, S. F., Haider, A. J., Al-Musawi, S., & Selman, M. K. 2024. Antibacterial effect of copper oxide nanoparticles prepared by laser production in water against staphylococcus aureus and Escherichia Coli. *Plasmonics*, *19*(5), 2401-2411.
24. Omran, B. A., Rabbee, M. F., Abdel-Salam, M.O., & Baek, K.H. 2025. Biogenically synthesized copper oxide, titanium oxide, and silver oxide nanoparticles: Characterization and biological effects. *Clean Technologies and Environmental Policy*, *27*(7), 2873-2898.
25. Yeap, S. P., Lim, J., Ngang, H. P., Ooi, B. S., & Ahmad, A. L. 2018. Role of particle–particle interaction towards effective interpretation of Z-average and particle size distributions from dynamic light scattering (DLS) analysis. *Journal of nanoscience and nanotechnology*, *18*(10), 6957-6964.